Microporous and Mesoporous Materials 116 (2008) 555–560

Contents lists available at ScienceDirect

Microporous and Mesoporous Materials

journal homepage: www.elsevier.com/locate/micromeso

Zeolites as supports for the biorecovery of hexavalent and trivalent chromium

Bruna Silva [a,*], Hugo Figueiredo [a], Cristina Quintelas [a], Isabel C. Neves [b], Teresa Tavares [a]

[a] IBB – Instituto de Biotecnologia e Bioengenharia, Centro de Engenharia Biológica, Universidade do Minho, Campus de Gualtar, 4710-057 Braga, Portugal
[b] Departamento de Química, Centro de Química, Universidade do Minho, Campus de Gualtar, 4710-057 Braga, Portugal

ARTICLE INFO

Article history:
Received 21 January 2008
Received in revised form 8 May 2008
Accepted 8 May 2008
Available online 15 May 2008

Keywords:
NaY
Arthrobacter viscosus
Biosorbents
Cr(VI)
Cr(III)

ABSTRACT

The aim of this study is the preparation and characterization of new catalytic materials to be used in oxidation reactions through the recovery of heavy metals in wastewater. The recovery of Cr(III) and Cr(VI) from aqueous solutions by an *Arthrobacter viscosus* biofilm supported on NaY zeolite was investigated. Experiments were repeated without the bacteria for comparison purposes. The batch method has been employed, using solutions with chromium concentrations of 10 mg L^{-1}, 25 mg L^{-1}, 50 mg L^{-1} and 100 mg L^{-1}. Cr(III) was easily removed from solution due to its positive charge which allows the entrapment in the framework zeolite by ion exchange. However, due to its anionic form Cr(VI) was only removed in the presence of the biofilm that performs its reduction to Cr(III), followed by ion exchange in the zeolite. The best uptake was achieved for initial concentration of 100 mg L^{-1}: 14 mg $g_{zeolite}^{-1}$ for Cr(III) by both systems and 3 mg $g_{zeolite}^{-1}$ for Cr(VI) by the zeolite with the bacterium biofilm. The modified zeolite samples have been fully characterized by surface analysis (XRD, XPS), chemical analyses (ICP-AES), spectroscopic method (FTIR) and microscopic analysis (SEM). The results show that the biofilm of *A. viscosus* supported on NaY zeolite is able to recover chromium from dilute solutions and the framework zeolite remains unchanged after chromium biosorption.

1. Introduction

Heavy metals released into the environment have been increasing continuously as a result of industrial activities and technological development, posing a significant threat to environment and public health because of their toxicity, accumulation in the food chain and persistence in nature [1].

Among the different heavy metals, chromium is one of the most toxic and is introduced into the environment through a variety of industrial activities. The major sources of contamination are electroplating, metal finishing industries and tanneries [2]. Chromium exists in oxidation states from +2 to +6, but only two states, +3 and +6, are of environmental significance [3]. These two oxidation states have widely contrasting toxicity and transport characteristics: hexavalent chromium is more toxic, with high water solubility and mobility, while trivalent chromium is less soluble in water, less mobile and less harmful [4–7]. The Cr(VI) species may be in the form of dichromate ($Cr_2O_7^{2-}$), hydrochromate ($HCrO_4^-$), or chromate (CrO_4^{2-}) in a solution of different pH values. Due to the repulsive electrostatic interactions, these Cr(VI) anion species are generally poorly adsorbed by the negatively charged soil particles and, hence, they can move freely in the aqueous environments. The Cr(III) species in aqueous solutions, however, may take the form of trivalent chromium $Cr(H_2O)_6^{3+}$ and chromium hydroxide complexes $Cr(OH)(H_2O)_5^{2+}$ or $Cr(OH)_2(H_2O)_4^+$, depending on the solution pH values. As these species normally carry positive electric charges, they can be easily adsorbed on the negatively charged soil particles and thus are less mobile than the Cr(VI) species in the environment [8].

Numerous processes exist for removing heavy metal ions from liquid solutions including chemical precipitation, chemical oxidation or reduction, ion exchange, membrane filtration and carbon adsorption [9]. However, these processes have significant disadvantages such as incomplete metal removal, high reagent or energy requirements, generation of toxic sludge or other waste products and are generally very expensive when the contaminant concentration is in the range (10–100) mg L^{-1} [10]. Cost effective alternative technologies or sorbents for treatment of metals contaminated waste streams are needed. A new system for chromium removal combines biosorption by a bacterium with the ion exchange capacity of a zeolite.

In recent years, the biosorption process has been studied extensively using microbial biomass as biosorbent for heavy metal removal. The major advantage of biosorption is evident particularly in the treatment of large volumes of effluents with low concentration of pollutants [1]. It is a promising process with a potential for industrial use and this is due to the ability of microorganisms to sorb metal ions, their suitability for natural environments and low cost. Generally, biosorption processes can reduce

* Corresponding author.
E-mail address: bsilva@deb.uminho.pt (B. Silva).

1387-1811/$ - see front matter © 2008 Elsevier Inc. All rights reserved.
doi:10.1016/j.micromeso.2008.05.015

capital costs by 20%, operational costs by 36% and total treatment costs by 28%, compared with conventional systems [11]. Biosorption is generally defined as the accumulation of metals by biological materials without active uptake and can be considered as a collective term for a number of passive accumulation processes which may include ion exchange, coordination, complexation, chelation, adsorption and microprecipitation [12]. On the other hand, metal uptake can also involve active metabolic passage across the cell membrane into the cell. This is referred to as active uptake. The combination of active and passive modes is called bioaccumulation. Metal uptake by dead cells takes place only by the passive mode. Living cells employ both active and passive modes for heavy metal uptake [7].

The use of bacteria for biosorption is a fast growing field in metal remediation because of their ubiquity, ability to grow under controlled conditions and small size [7]. The bacterium used in this work, *Arthrobacter viscosus*, is a good exopolysaccharide producer, which by itself allows foreseeing good qualities for support adhesion and for metal ions entrapment [13].

Various treatment processes are available for heavy metals removal, among which ion exchange is considered to be cost effective if low cost ion exchangers such as zeolites are used [14]. Zeolites are hydrated aluminosilicate materials having connected cage-like or channel structures with internal and external surface areas of up to 900 $m^2\,g^{-1}$. The structures of zeolites consist of three-dimensional frameworks of SiO_4 and AlO_4 tetrahedra. The aluminium ion is small enough to occupy the position in the center of the tetrahedron of four oxygen atoms and the isomorphous replacement of Si^{4+} by Al^{3+} produces a negative charge in the lattice. The net negative charge is balanced by the exchangeable cation (sodium, potassium or calcium). The fact that zeolite exchangeable ions are relatively innocuous makes them particularly suitable for removing undesirable heavy metal ions from industrial liquid effluents [15]. Due to their negative charge, zeolites have a strong affinity for transition metal cations, but only little affinity for anions and non-polar organic molecules [16]. This may be changed by surface pre-treatment or surface coverage by a specific biofilm [17]. Santiago et al. [18] reported unaltered zeolite to be ineffective for Cr(VI) removal and investigated the use of zeolites tailored with the organic cations ethylhexadecyldimethylammonium (EHDDMA) and cetylpyridinium (CETYL). Tailoring of the zeolite results in a positively charged species, allowing the anion exchange in which CrO_4^{2-} attaches to the tailored zeolite. Adsorption capacities of approximately 0.65 $mg\,g_{zeolite}^{-1}$ and 0.42 $mg\,g_{zeolite}^{-1}$ were achieved respectively with CETYL with EHDDMA. Alternatively, recent studies have shown that certain species of bacteria are capable of transforming hexavalent chromium, Cr(VI), into the much less toxic and less mobile trivalent form, Cr(III) [19–22,4]. Bacteria may protect themselves from toxic substances in the environment by transforming toxic compounds through oxidation, reduction or methylation into more volatile, less toxic or readily precipitating forms. In the present work, *A. viscosus* bacterium supported on the zeolite performs the reduction of Cr(VI) to Cr(III), and then the Cr(III) is retained in the zeolite by ion exchange. In this way, the bacteria allow metal loading of the zeolite, as sterical limitations and charge repulsions would not permit the zeolite loading with the anionic species, $Cr_2O_7^{2-}$ [23].

The aim of the present work was to investigate the recovery of metallic ions from aqueous solutions of Cr(VI) and Cr(III) by an *A. viscosus* biofilm supported on NaY zeolite. For performance comparison, the same study was carried out without the bacterium biofilm. After the biosorption process, the modified zeolites can be used as competitive and selective catalysts to be applied in catalytic oxidations of volatile organic compounds, as reported in previous work [23].

2. Experimental

2.1. Materials and reagents

Arthrobacter viscosus was obtained from the Spanish Type Culture Collection of the University of Valencia. Aqueous chromium trichloride solutions and aqueous potassium dichromate solutions were prepared by diluting $CrCl_3{\cdot}6H_2O$ (Merck) and $K_2Cr_2O_7$ (Panreac) in distilled water. The faujasite zeolite NaY (Si/Al = 2.83) with specific surface area of 900 $m^2\,g^{-1}$, was obtained from Zeolyst. It was calcined at 500 °C during 8 h under a dry air stream prior to use.

All glassware used for experimental purposes was washed in 10% nitric acid to remove any possible interference by other metals. Atomic absorption spectrometric standards were prepared from 1000 $mg\,L^{-1}$ solution.

2.2. Methods

2.2.1. Preparation of the biofilm supported on zeolites

A medium with 10 $g\,L^{-1}$ of glucose, 5 $g\,L^{-1}$ of peptone, 3 $g\,L^{-1}$ of malt extract and 3 $g\,L^{-1}$ of yeast extract was used for the microorganism growth. The medium was sterilized at 121 °C for 20 min, cooled to room temperature, inoculated with bacteria and kept at 28 °C for 24 h with moderate stirring in an incubator. Then, batch experiments were conducted using 1 g of the NaY zeolite with 15 mL of *A. viscosus* culture media and 150 mL of the different potassium dichromate solutions and chromium chloride solutions (10, 25, 50 and 100) $mg\,L^{-1}$ in 250 mL Erlenmeyer flasks. Experiments were repeated without the bacterium for comparison purposes. All experimental work was conducted in duplicate. The Erlenmeyer flasks were kept at 28 °C, with moderate stirring for about 10 days. Samples of 1 mL were taken, centrifuged and analyzed for metals using atomic absorption spectrophotometry. After the experimental studies, the solid samples were centrifuged and dried at 60 °C for 3 days. They have been identified by designation $Cr(m)_n$–Y or $^*Cr(m)_n$–Y, where symbol * represents the zeolite samples without the bacterium biofilm, m the oxidation state of chromium and n the initial concentration of chromium in the solution. For some characterization analyses the samples were calcined using the same procedure described above.

2.2.2. Characterization procedures

Total metal ions concentrations during the experiments were measured using a Varian Spectra AA-400, an Atomic Absorption Spectrophotometer (AAS) operated in flame mode, with direct aspiration. Room temperature FTIR spectra of zeolite samples were obtained from powdered samples on KBr pellets, using a Bomem MB104 spectrometer in the 4000–500 cm^{-1} range by averaging 20 scans at a maximum resolution of 10 cm^{-1}. Powder X-ray diffraction patterns (XRD) were recorded using a Philips Analytical X-ray model PW1710 BASED diffractometer system. Scans were taken at room temperature, using CuKα radiation in a 2θ range between 5° and 70°. The morphology and particle size of zeolite samples were evaluated by Scanning Electron Microscopy (SEM), using a Leica Cambridge S360. Solid samples were coated with Au in vacuum to avoid surface charging using a Fisons Instruments SC502 sputter coater. The samples with bacteria were previously dehydrated with ethanol. Elemental chemical analyses (Si, Al, Na and Cr) were performed by Inductively Coupled Plasma Atomic Emission Spectrometry (ICP-AES) using a Philips ICP PU 7000 Spectrometer on samples. X-ray photoelectron spectroscopy analyses were obtained in a VG Scientific ESCALAB 250iXL spectrometer using a monochromatic AlKα radiation at 1486.92 eV. In order to correct possible deviations caused by electric change of the

samples, the C 1 s line at 285.0 eV was taken as internal standard [24,25].

3. Results and discussion

3.1. Uptake studies

The removal of Cr(III) and Cr(VI) by NaY zeolite with and without the bacterium biofilm showed similar profiles for all range of initial concentrations. As an example, in Fig. 1 are shown the removal ratios of the metallic ions for initial concentrations of 10 mg L^{-1} and 50 mg L^{-1}.

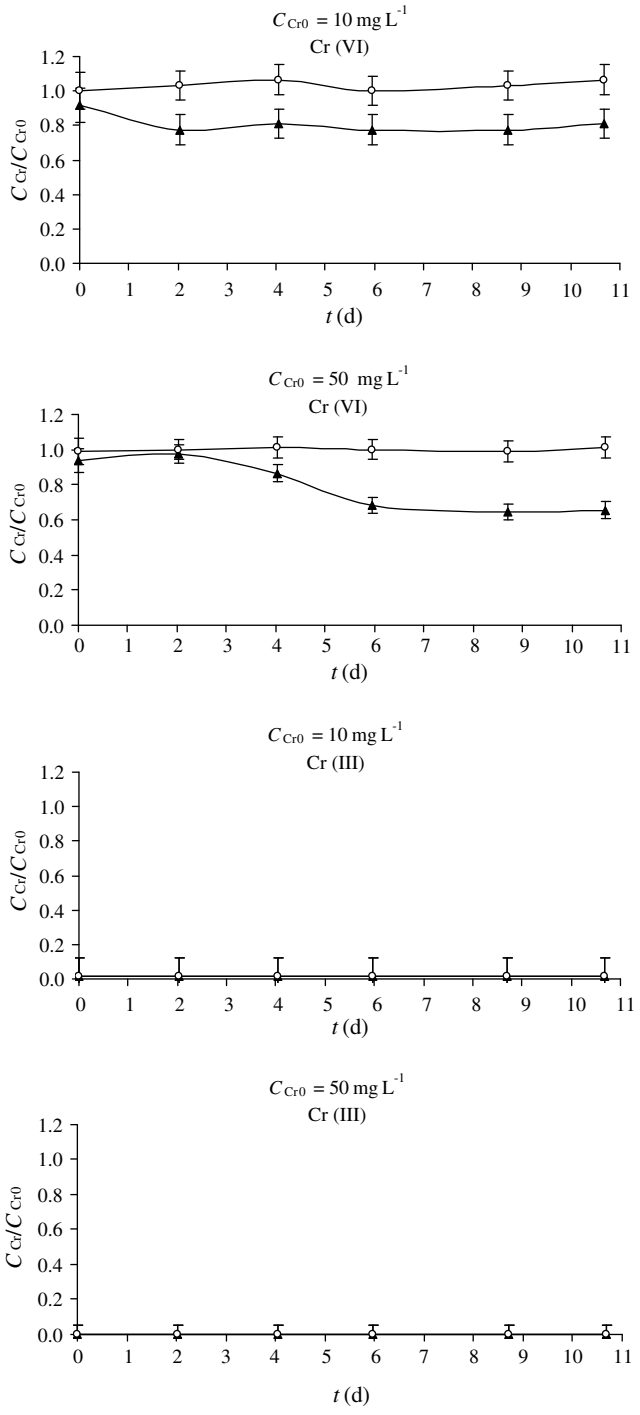

Fig. 1. Ratio between residual and initial chromium concentration (C_{Cr}/C_{Cr0}) as a function of contact time, for initial concentrations of Cr(VI) and Cr(III) of 10 mg L^{-1} and 50 mg L^{-1}, in the presence of the zeolite with (▲) and without the bacteria (○).

The removal of chromium by the conjugated system (biofilm/zeolite) presented a typical and well known biosorption kinetics [13], which includes two phases: the first one, very fast and not observable in Fig. 1, but determined by mass balance, is associated with the external cell surface, biosorption itself, and the second one is an intra-cellular accumulation/reaction, depending on the cellular metabolism [26]. The results showed that Cr(III) was completely removed by both systems, due to the affinity between the positive charge of the metal and the negative charge of the bacteria and to the easiness of entrapment in the framework zeolite by ion exchange. Contrarily, the zeolite was not able to remove Cr(VI) which is related with its anionic form. The peculiar adsorptive properties of zeolites are due to the negative charge of the framework Al atoms, which are located inside the three-dimensional pore structure of the solid. However, in the presence of the bacterium biofilm, the removal efficiency was flagrantly improved by 19% for initial concentration of 10 mg L^{-1} and by 35% for initial concentration of 50 mg L^{-1}, as shown in Fig. 1. The role of the biofilm is the reduction of Cr(VI) to a smaller cation, Cr(III), being this ion easily exchanged in the internal surface of the zeolite. The reduction can only occur on the outer surface of the zeolite as $Cr_2O_7^{2-}$ is not able to get inner the zeolite framework [23]. The lower removal ratios of Cr(VI) compared to Cr(III) seem to be connected with the lack of affinity between the global charge of the bacteria and the metallic ion, the charge repulsions with the zeolite as well as with the sterical effects due to a higher ionic radius. As it is well known, Y zeolite structure presents a large central cavity or supercage with a diameter of 12.5 Å, sharing the supercages a 12-membered ring with an open diameter of 7.4 Å [27]. In terms of ionic dimensions, trivalent chromium in the form of $Cr(H_2O)_6^{3+}$ has an ionic radius of 4.8 Å whereas $Cr_2O_7^{2-}$ presents a dimension of 6.2 Å (calculations performed by using CAChe program, Oxford Molecular, 1997). In addition, there are probably limitations in the extension of the adhesion of *A. viscosus* to the support, as the characteristic dimension of bacteria ranges from 1 to 10 μm. Although Y zeolite exhibits large specific surfaces areas, typically higher than 700 $m^2\ g^{-1}$, most of this area is internal with an internal void volume above 0.1 $cm^3\ g^{-1}$ [27].

Fig. 2 shows the dependence of the total uptake of Cr(VI) and Cr(III) as a function of the initial concentration in the solution.

For both metallic ions there is an increase of uptake with the increasing of the initial concentration. For this concentration range and experimental conditions the effect of the increasing driving force due to higher concentrations was probably predominant over the saturation of the matrix surface. Thus, the best uptake was achieved for initial concentration of 100 mg L^{-1}: 14 mg $g^{-1}_{zeolite}$ for Cr(III) by both systems and 3 mg $g^{-1}_{zeolite}$ for Cr(VI) by zeolite covered with the bacterium biofilm.

3.2. Materials characterization

The solid samples obtained after the experiments were characterized by surface analysis (XRD, XPS), chemical analyses (ICP-AES), spectroscopic method (FTIR) and microscopic analysis (SEM).

The XRD patterns of the NaY zeolite and the modified zeolite samples with chromium are very similar and the sample $Cr(VI)_{50}$–Y has been chosen as an example. In Fig. 3 is described the diffractograms of NaY (A) and $Cr(VI)_{50}$–Y (B). The similarity between the diffractograms of the modified zeolite samples after chromium biosorption and the original one reveals that this process does not promote any structural modification in the NaY zeolite. The diffractograms also show no peaks due to chromium, probably because of its very low percent loading.

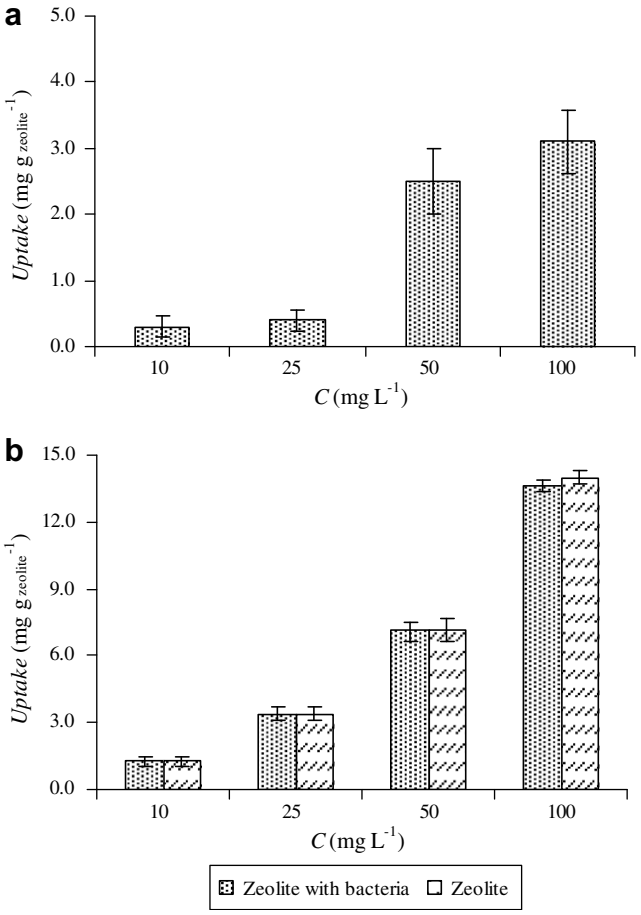

Fig. 2. Uptake of Cr(VI) (a) and Cr(III) (b), in terms of zeolite mass, as a function of the initial concentration of metal in solution, in the presence of zeolite with and without the bacterium biofilm.

Table 1 summarizes the structural properties of the starting NaY and the Cr_{50}–Y/$^{*}Cr_{50}$–Y zeolite samples, obtained by XRD patterns. The unit cell parameters (a_0) were calculated from the [533], [642] and [555] reflection peak positions that were determined using the [101] reflection of the quartz ($2\theta = 26.64187°$) as an internal standard by ASTM D 3942-80. The relative crystallinity was estimated by comparing the peak intensities of the modified zeolites samples with those of starting NaY (100% of crystallinity).

Table 1
Structural and chemical analysis of zeolite samples

Sample	a_0 (Å)[a]	Crystal size (nm)	Relative crystallinity (%)[b]	Si/Al_{bulk}[c]	Cr (%)[c]
NaY	24.626	9	100	2.83	–
$^{*}Cr(III)_{50}$–Y	24.661	10	71	2.84	0.55
$Cr(III)_{50}$–Y	24.656	8	67	2.84	0.52
$^{*}Cr(VI)_{50}$–Y	24.667	9	67	2.82	<0.01
$Cr(VI)_{50}$–Y	24.670	9	68	2.81	0.25

[*] Samples without bacterium biofilm.
[a] a_0 is the unit cell parameter determined from XRD analysis.
[b] Comparison with NaY by XRD analysis.
[c] Bulk Si/Al ratio and Cr content determined from ICP-AES.

The results reveal that the a_0 lattice parameter was relatively unaffected after the removal of metallic ions, showing at most an expansion of 0.18%.

The total intensities of the six peaks assigned to [331], [511], [440], [533], [642], and [555] reflections were used for the comparison according to ASTM D3906 method [28]. The results show that the zeolites loaded with chromium maintained about 70% of crystallinity as compared to the respective standard NaY zeolite (Table 1).

Crystal sizes were estimated from the most intense reflection peak [555] by XRD line broadening using the Scherrer equation (Eq. (1)), where D is the crystal size, K is a constant (0.9), λ the X-ray wavelength, B the peak with at a half-height and 2θ the position of the [hkl] reflection.

$$D = \frac{K\lambda}{B\cos\theta} \quad (1)$$

The [555] reflection for zeolite samples was fitted by a Gaussian profile to determine the peak widths at half-height. The crystal sizes of the standard NaY and those of modified zeolite samples are similar (Table 1), ranging between 8 nm and 10 nm, which is a further evidence of the maintenance of zeolite structure. Thus, the uptake process described in this work did not modify significantly the zeolite structure.

As indicated in addition in Table 1, the results of Cr elemental analysis show that the biosorption process allowed the retention of chromium in the NaY zeolite. The molar Si/Al ratio for all samples did not change substantially after the biosorption process which indicates that no dealumination occurred during this treatment. The expected higher amount of Cr observed after exchange with aqueous chromium chloride solution is confirmed when compared with the uptake process. In this case, chromium is in the

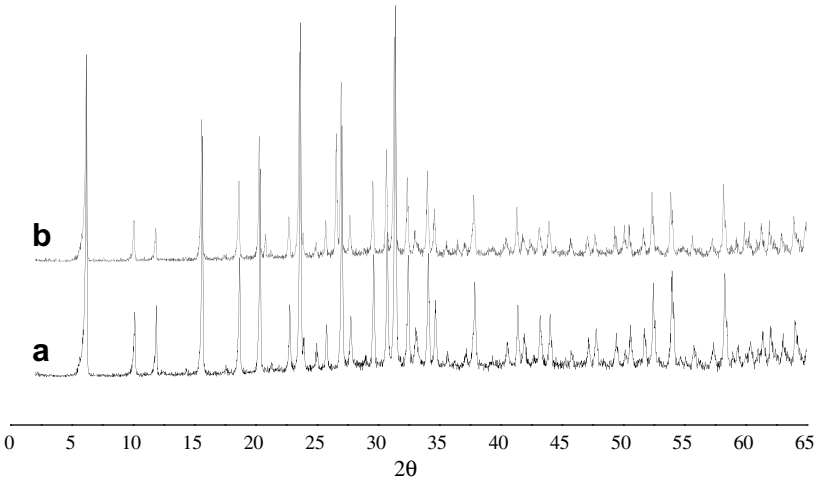

Fig. 3. XRD patterns of NaY (a) and $Cr(VI)_{50}$–Y (b).

Cr(III) form, a smaller cation and this ion is easily exchanged within the zeolite.

The morphology of the starting NaY and of the zeolite samples after the uptake process was evaluated by SEM. Fig. 4 shows SEM photographs of NaY, $^{*}Cr(VI)_{100}$–Y, $Cr(VI)_{10}$–Y and $^{*}Cr(VI)_{10}$–Y.

The bacterium biofilm on the zeolite surface with a considerable production of exopolysaccharide that provides a good adhesion to the support may be seen in Fig. 4c. The average dimension of the bacteria was in the range between 1 μm and 1.5 μm, while the particle size of all zeolite samples was about of 0.5–1 μm. The comparison of the photographs of NaY and modified zeolite samples indicates that the particle size and morphology remained unchanged after the fixation of chromium ions.

Furthermore, structural information of zeolite samples was obtained by FTIR spectroscopy. It was found that the FTIR spectra of NaY and $Cr(m)_n$–Y/$^{*}Cr(m)_n$–Y samples were very similar and the samples $Cr(VI)_{50}$–Y/$^{*}Cr(VI)_{50}$–Y have been chosen as an example. The FTIR spectra in the range (4000–500) cm^{-1} are presented in Fig. 5 for the starting NaY, $Cr(VI)_{50}$–Y, $^{*}Cr(VI)_{50}$–Y and *A. viscosus* bacterium.

The spectra of NaY zeolite and modified zeolite samples are dominated by strong zeolite bands: the broad band at (3700–3300) cm^{-1} is attributed to surface hydroxyl groups and bands corresponding to the lattice vibrations are observed in the spectral region between 1300 cm^{-1} and 450 cm^{-1} [29]. No shift or broadening of the NaY zeolite vibrations are observed upon inclusion of chromium by the biosorption process, which provides further evidence that the framework zeolite remains unchanged.

The infrared spectrum of the *A. viscosus* bacterium (Fig. 5 – spectrum d) is typical from bacterial extracellular polymeric substances with a complex mixture of macromolecular polyelectrolytes including polysaccharides, proteins, nucleic acids [30] and lipids or humic substances [31]. The FTIR spectrum shows one broad band in 3300 cm^{-1} due to the vibrations of hydroxyl and amide (N–H stretching) groups; the small bands in the range between 2970 cm^{-1} and 2800 cm^{-1} are attributed to C–H stretching of the groups CH_2 and CH_3; the characteristic region of the bands between 1650 cm^{-1} and 1400 cm^{-1} are attributed to the vibrations of the functional groups such as carboxyl, phosphoric,

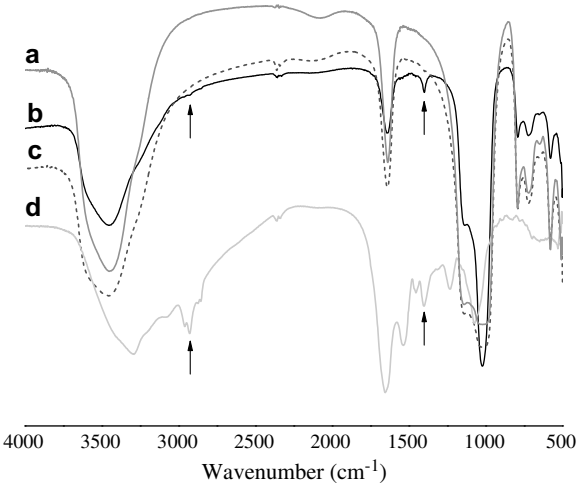

Fig. 5. FTIR spectra in the range (4000–500) cm^{-1} for: NaY (a), $Cr(VI)_{50}$–Y (b), $^{*}Cr(VI)_{50}$–Y (c) and *A. viscosus* bacterium (d).

amine and the bands in the frequency range 1250–900 cm^{-1} result from vibrations of the polysaccharides from the bacterium [30–32]. In the $Cr(VI)_{50}$–Y spectrum (Fig. 5 – spectrum b), the presence of the organic material can be only detected by a band at 1400 cm^{-1} and a weak band at 2925 cm^{-1},where the zeolite does not absorb.

The XPS technique, which allows an analysis of the inner structure and cavity contents up to a depth of about 50 Å [29] can provide information about the presence of chromium through the surface layer of NaY as well as about the oxidation state of the metal. All samples revealed the presence of sodium, silicon and aluminium in their XPS resolution spectra. The presence of chromium was detected in the modified zeolite spectra. It was also detected carbon and nitrogen from the organic matter in the samples with *A. viscosus* before calcination. Table 2 presents the XPS analysis based on C 1s, N 1s, Na 1s, Al 2p, Si 2p and Cr 2p peak intensities for NaY, $^{*}Cr(III)_{50}$–Y, $Cr(III)_{50}$–Y and $Cr(VI)_{50}$–Y samples, before and after calcination.

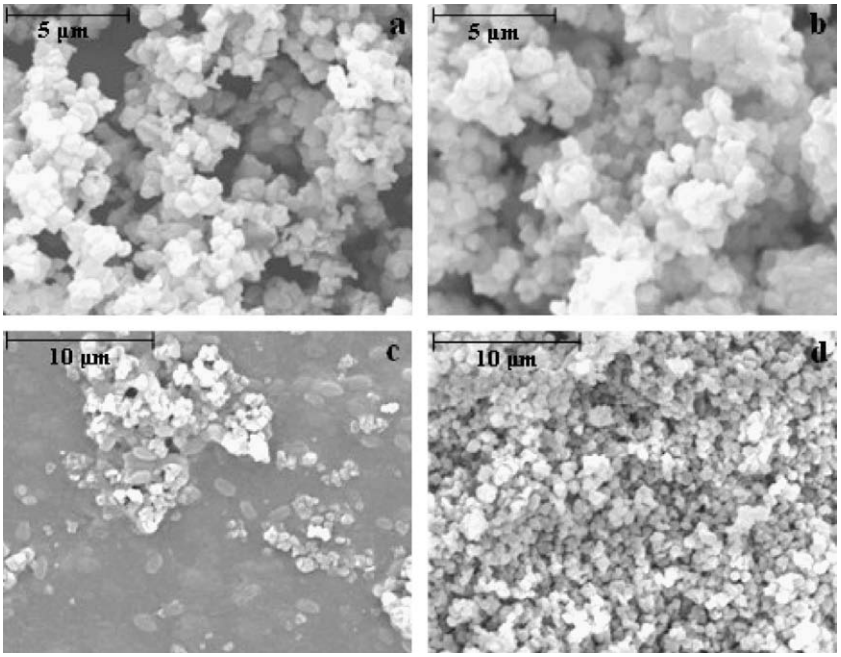

Fig. 4. SEM of NaY zeolites (a) (5000×), $^{*}Cr_{100}$–Y (b) (5000×), Cr_{10}–Y (c) (3000×) and $^{*}Cr_{10}$–Y (d) (3000×).

Table 2
Elemental analysis as determined by XPS

Sample	XPS (atom%)						Si/Al	Cr/Si	Cr/Al
	Si	Al	Na	Cr	C	N			
NaY	23.8	7.4	11.4	–	–	–	3.10	–	–
*Cr(III)$_{50}$–Y	23.7	6.3	6.9	0.3	–	–	3.76	0.013	0.048
*Cr(III)$_{50}$–Y[a]	25.1	6.5	5.5	0.1	–	–	3.86	0.004	0.015
Cr(III)$_{50}$–Y	20.2	6.2	5.5	0.9	14.8	2.3	3.26	0.045	0.145
Cr(III)$_{50}$–Y[a]	24.6	6.7	6.2	0.5	–	–	3.67	0.020	0.075
Cr(VI)$_{50}$–Y	20.6	6.4	5.7	0.3	14.5	2.3	3.22	0.015	0.047
Cr(VI)$_{50}$–Y[a]	24.3	6.3	5.4	0.0	–	–	3.86	0.000	0.000

* Samples without bacterium biofilm.
[a] Samples after calcination.

The results reveal that there is a strong reduction of chromium concentration on the zeolite surface after the calcination. This decrease is due to the migration of metallic ions into the zeolite matrix during the calcination process [33,34]. This is an important step to future use of these modified zeolites as competitive and selective catalysts to be applied in catalytic oxidations of organic compounds, as reported in previous work [23,34]. The Si/Al ratios of the external surface measured by XPS show that the NaY surface is rich in silicon groups. The difference between the Si/Al ratios determined at surface by XPS (Table 2) and those determined in bulk by chemical analysis (Table 1) indicates an uneven distribution of silicon and aluminium throughout the zeolite structure.

For Cr(III)$_{50}$–Y sample, the amount of Cr from XPS is very similar to the bulk chromium content (Tables 1 and 2). Chromium is homogeneously distributed throughout the NaY structure. However, in absence of the bacteria, *Cr(III)$_{50}$–Y, the amount of chromium after calcination is lower than total Cr determined by chemical analyses. The calcination provokes the migration of Cr into the NaY structure. XPS analysis detects a higher amount of Cr in surface before calcination and after calcination the Cr diffuses into the structure.

The binding energies of the peaks in the Cr 2p region of the modified zeolites were obtained for Cr(VI)$_{50}$–Y and Cr(III)$_{50}$–Y samples. The reference values of the binding energy for Cr^{3+} in the Cr $2p_3$ region is 576–576.6 eV, 577.5–577.3 eV [35] and 575.6 eV [36]. Before calcination, the Cr 2p spectrum of the Cr(VI)$_{50}$–Y sample shows a peak for the Cr $2p_3$ region at the binding energy of 576.6 eV. This value confirms that the metal is in oxidation state three [35], in agreement with the previous assumptions. Thus, Cr(VI) was effectively reduced to Cr(III) by the bacterium biofilm before the entrapment in the zeolite. After calcination treatment, the chromium was not detected in this sample (Table 2). Before calcination, for Cr(III)$_{50}$–Y and *Cr(III)$_{50}$–Y samples peaks at the binding energies of 575.71 eV and 575.85 eV are observed, which indicates that the metal is in oxidation state three [36] as in the starting solution. After calcination, these samples show the peaks at the binding energies of 577.14 eV and 577.13 eV. The increase in value of the binding energy of the Cr^{+3} species suggests stronger interactions with the zeolite framework due to the calcination treatment.

4. Conclusion

A biofilm of *A. viscosus* supported on NaY zeolite is able to recover Cr(VI) and Cr(III) from dilute solutions. Cr(III) was easily removed from solution due to its positive charge which allows the entrapment in the framework zeolite by ion exchange. Contrarily, due to its anionic form Cr(VI) was only removed in the presence of the biofilm that performs its reduction to Cr(III), followed by ion exchange in the zeolite. By combining data from the different techniques used it is possible to confirm that the biosorption process does not cause damage on the morphology and structure of the NaY zeolite, which has especially importance in further utilization of these materials as catalysts for VOC's oxidation.

Acknowledgments

Dr. C.S. Rodriguez (C.A.C.T.I., Vigo University, Spain) is gratefully acknowledged for performing and interpreting the XPS analyses. We thank Dr. A.S. Azevedo (Departamento de Ciências da Terra, Minho University) for collecting the powder diffraction data. This work was supported by Fundação para a Ciência e Tecnologia (FCT-Portugal), under programme POCTI/FEDER (POCTI/44449/CTA/2002) and POCTI-SFA-3-686. B.S. and H.F. thank FCT for a Ph.D. Grant.

References

[1] M. Gavrilescu, Eng. Life Sci. 4 (3) (2004) 219.
[2] G.S. Agarwal, H.K. Bhuptawat, S. Chaudhhari, Bioresour. Technol. 97 (2005) 949.
[3] M. Ghiaci, R. Kia, A. Abbaspur, F. Seyedeyn-Azad, Sep. Purif. Technol. 40 (2004) 285.
[4] T.L. Kalabegishvili, N.Y. Tsibakhashvili, H.-Y.N. Holman, Environ. Sci. Technol. 37 (2003) 4678.
[5] N.Y. Tsibakhashvili, L.M. Mosulishvili, T.L. Kalabegishvili, E.I. Kirkesali, M.V. Frontasyeva, E.V. Pomyakushina, S.S. Pavlov, H.-Y.N. Holman, J. Radioanal. Nucl. Chem. 259 (3) (2004) 527.
[6] Z. Lin, Y. Zhu, T.L. Kalabegishvili, N.Y. Tsibakhashvili, H.-Y. Holman, Mater. Sci. Eng. C-Bio. S. 26 (2006) 610.
[7] D. Mohan, C.U. Pittman Jr., J. Hazard. Mater. B 137 (2006) 762.
[8] S. Deng, R. Bai, Water Res. 38 (2004) 2424.
[9] S.E. Bailey, T.J. Olin, R.M. Bricka, D.D. Adrian, Water Res. 33 (11) (1999) 2469.
[10] Y. Sağ, T. Kutsal, Chem. Eng. J. 60 (1995) 181.
[11] M.X. Loukidou, A.I. Zouboulis, T.D. Karapantsios, K.A. Matis, Colloid Surf. A 242 (2004) 93.
[12] J.R. Duncan, D. Brady, A. Stoll, Environ. Technol. 15 (1994) 429.
[13] C. Quintelas, T. Tavares, Biotechnol. Lett. 23 (2001) 1349.
[14] V.J. Inglezakis, M.D. Loizidou, H.P. Grigoropoulou, J. Colloid Interface Sci. 261 (2003) 49.
[15] E. Erdem, N. Karapinar, R. Donat, J. Colloid Interface Sci. 280 (2004) 309.
[16] M.V. Mier, R.L.P. Callejas, R. Gehr, B.E.J. Cisneros, P.J.J. Alvarez, Water Res. 35 (2) (2001) 373.
[17] M.T. Tavares, C. Quintelas, H. Figueiredo, I.C. Neves, Mater. Sci. Forum 514–516 (2006) 1294.
[18] I. Santiago, V.P. Worland, E. Cazares-Rivera, F. Cadena, in: 47th Purdue Industrial Waste Conference Proceedings, vol. 669, 1992.
[19] K.H. Cheung, J.-D. Gu, Chemosphere 52 (2003) 1523.
[20] H. Guha, K. Jayachandran, F. Maurrasse, Chemosphere 52 (2003) 175.
[21] E. Dermou, A. Velissariou, D. Xenos, D.V. Vayenas, J. Hazard. Mater. B 126 (2005) 78.
[22] S.-Y. Kang, J.-U. Lee, K.-W. Kim, Biochem. Eng. J. 36 (2007) 54.
[23] H. Figueiredo, I.C. Neves, C. Quintelas, T. Tavares, M. Taralunga, J. Mijoin, P. Magnoux, Appl. Catal., B-Environ. 66 (2006) 273.
[24] J.Y. Xie, P.M.A. Sherwood, Chem. Mater. 2 (3) (1990) 293.
[25] J.F. Moulder, W.F. Strickle, P.E. Sobol, K.D. Bomben, in: J. Chastain (Ed.), Handbook of X-ray Photoelectron Spectroscopy, Perkin Elmer, Eden Prairie, Minnesota, 1992, p. 10.
[26] M.T. Tavares, C. Martins, P. Neto, in: A.K. Sengupta (Ed.), Hazardous and Industrial Wastes, Tecnomics Publishing Co., Lancaster, 1995, p. 223.
[27] A. Corma, Chem. Rev. 95 (1995) 559.
[28] I.C. Neves, G. Botelho, A.V. Machado, P. Rebelo, Eur. Polym. J. 42 (2006) 1541.
[29] B. Imelik, J.C. Vedrine (Eds.), Catalyst Characterization: Physical Techniques for Solid Materials, Plenum Press, New York, 1994, p. 11.
[30] A. Omoike, J. Chorover, Biomacromolecules 5 (2004) 1219.
[31] M.H. Zandvoort, P.N.L. Lens, E. van Hullebusch, L. Lettinga, Soil Sediment Contam. 12 (5) (2003) 679.
[32] T. Udelhoven, D. Naumann, D. Schmitt, Appl. Spectrosc. 54 (2000) 1471.
[33] S.J. Kulkarni, S.B. Kulkarni, Thermochim Acta 56 (1) (1982) 93.
[34] H. Figueiredo, B. Silva, M.M.M. Raposo, A.M. Fonseca, I.C. Neves, C. Quintelas, T. Tavares, Microporous Mesoporous Mater. 109 (2008) 163.
[35] L. Cunha, M. Andritschky, L. Rebouta, K. Pischow, Surf. Coat. Technol. 116–119 (1999) 1152.
[36] Handbook of the Elements and Native OxidesBE Lookup Table for Signals from Elements and Common Chemical Species, XPS International Inc., 1999. available at: <http://www.xpsdata.com>.